On the influence of the diurnal variations of aerosol content to estimate direct aerosol radiative forcing using MODIS data

Hui Xu, Jianping Guo, Xavier Ceamanos, Jean-Louis Roujean, Min Min, Dominique Carrer

On the influence of the diurnal variations of aerosol content to estimate direct aerosol radiative forcing using MODIS data

Hui Xu [a], Jianping Guo [a, *], Xavier Ceamanos [b], Jean-Louis Roujean [c], Min Min [d], Dominique Carrer [c]

[a] State Key Laboratory of Severe Weather, Chinese Academy of Meteorological Sciences, Beijing 100081, China
[b] ONERA, The French Aerospace Lab, Toulouse 31055, France
[c] CNRM-GAME (UMR 3589), Météo-France/CNRS, Toulouse 31057, France
[d] National Satellite Meteorological Center, Chinese Meteorological Administration, Beijing 100081, China

Long-term measurements of aerosol optical depth (AOD) from the Aerosol Robotic Network (AERONET) located in Beijing reveal a strong diurnal cycle of aerosol load staged by seasonal patterns. Such pronounced variability is matter of importance in respect to the estimation of daily averaged direct aerosol radiative forcing (DARF). Polar-orbiting satellites could only offer a daily revisit, which turns in fact to be even much less in case of frequent cloudiness. Indeed, this places a severe limit to properly capture the diurnal variations of AOD and thus estimate daily DARF. Bearing this in mind, the objective of the present study is however to evaluate the impact of AOD diurnal variations for conducting quantitative assessment of DARF using Moderate Resolution Imaging Spectroradiometer (MODIS) AOD data over Beijing. We provide assessments of DARF with two different assumptions about diurnal AOD variability: taking the observed hourly-averaged AOD cycle into account and assuming constant MODIS (including Terra and Aqua) AOD value throughout the daytime. Due to the AOD diurnal variability, the absolute differences in annual daily mean DARFs, if the constant MODIS/Terra (MODIS/Aqua) AOD value is used instead of accounting for the observed hourly-averaged daily variability, is 1.2 (1.3) Wm^{-2} at the top of the atmosphere, 27.5 (30.6) Wm^{-2} at the surface, and 26.4 (29.3) Wm^{-2} in the atmosphere, respectively. During the summertime, the impact of the diurnal AOD variability on seasonal daily mean DARF estimates using MODIS Terra (Aqua) data can reach up to 2.2 (3.9) Wm^{-2} at the top of the atmosphere, 43.7 (72.7) Wm^{-2} at the surface, and 41.4 (68.8) Wm^{-2} in the atmosphere, respectively. Overall, the diurnal variation in AOD tends to cause large bias in the estimated DARF on both seasonal and annual scales. In summertime, the higher the surface albedo, the stronger impact on DARF at the top of the atmosphere caused by dust and biomass burning (continental) aerosol. This indicates that the impact on DARFs estimates is sensitive to assumptions of aerosol type and surface albedo.

1. Introduction

Atmospheric aerosols affect the Earth's energy budget directly by scattering and absorbing the solar radiation. Known as direct aerosol radiative forcing (DARF), these interactions are found to

* Corresponding author. Chinese Academy of Meteorological Sciences, 46 Zhong-Guan-Cun South Avenue, Haidian District, Beijing 100081, China.
E-mail address: jpguo@camscma.cn (J. Guo).

make a significant contribution to climate (e.g., Kaufman et al., 2002; Ramanathan et al., 2007; Guo et al., 2014; Wang et al., 2015a), affect regional atmospheric circulation (e.g., Ramanathan and Carmichael, 2008; Yoon et al., 2005), or even delay the onset of precipitating systems (Guo et al., 2016). In the assessment report of IPCC (2013), the scientific understanding of DARF has been designated as "High". However, estimates of DARF regionally still contain significant uncertainties due to complex aerosol sources, strong diurnal variability, and poorly known morphology (Arola et al., 2013). Reducing these uncertainties requires improved understanding of the spatial and temporal distribution of aerosols properties, such as aerosol optical depth (AOD, Adhikary et al., 2008), single scattering albedo (SSA) and asymmetry factor (ASY).

As satellite remote sensing remains the only means of observing the large spatial and temporal variability in aerosol properties, satellite observations have been used extensively to perform global estimates of DARF (Chin et al., 2009; Yu et al., 2006). Based on remote sensing observations, especially Moderate Resolution Imaging Spectroradiometer (MODIS) observations, significant advances have been made in quantifying the DARF under clear-sky conditions (Yu et al., 2006). However, MODIS acquires data over a same site twice per day due to the limited satellite revisit cycle, and thus the lack of fine temporal samplings of AOD from MODIS cannot allow us to faithfully reproduce the diurnal variations of AOD (Kuang et al., 2015).

The diurnal variability in aerosol burden can be quite significant (Smirnov et al., 2002; Eck et al., 2003; Zhang et al., 2012; Yin and Min, 2013). For example, Wang et al. (2015a, b) reported that diurnal changes of AOD can reach up to 0.54 during a highly polluted day in Hefei. The diurnal variations of AOD dramatically impact calculations of DARF (Christopher et al., 2003). Arola et al. (2013) reported that there can be significant biases in DARF estimates in individual sites if the constant AOD value for the daily mean was taken from the MODIS Terra or Aqua overpass times instead of accounting for the true observed daily variability. The AOD cycles with either maximum or minimum AOD close to local noon caused the most significant effect on daily DARF due to the impact of diurnal AOD variability. It has been shown by Wang et al. (2015b) that strong diurnal changes in aerosol loadings have an impact on the 24-h averaged DARF with reported absolute errors varying between −7.6 and 15.6 Wm^{-2}. However, diurnal variations of these optical properties have rarely been taken into account in the estimates of DARF using MODIS data.

The objective of this study is to investigate the influence of AOD diurnal variations on the estimation of DARF using MODIS data. Here we will focus on the Beijing site located in North China Plain where the aerosol loading is known to be very high. The descriptions of the ground-based and satellite measurements, as well as the methodologies used in this study, are given in Section 2. In Section 3, we present the diurnal variations in hourly mean AOD, the effects of seasonal and annual aerosol diurnal variations on the estimate of DARF, and the sensitivity of surface albedo and aerosol types to clear-sky DARF. Section 4 summarizes and concludes the study.

2. Materials and methods

2.1. Site description and measurements

The Beijing observation station (39.98°N, 116.38°E, 92 m) is situated at the northern tip of the North China Plain (Fig. 1). The climate of Beijing is known as "continental monsoon" and has four distinct seasons each year, i.e., winter (December, January and February; DJF), spring (March, April and May; MAM), summer (June, July and −August; JJA), and autumn (September, October and November; SON). Spring is occasionally impacted by the dust episode transported by northwesterly and westerly winds from the Kumutage and Taklimakan deserts in western China or by northerly winds from Mongolian deserts (Guo et al., 2013; Sun et al., 2001). In summer, it is characterized by relatively hot and humid weather and accounts for about 74% of annual precipitation (Yu et al., 2009). Autumn is relatively clean and clear and winter is windy and dry. In recently years, this region was plagued by deteriorated air quality due to the high aerosol emissions caused by rapid ecomonic development (Guo et al., 2009, 2011).

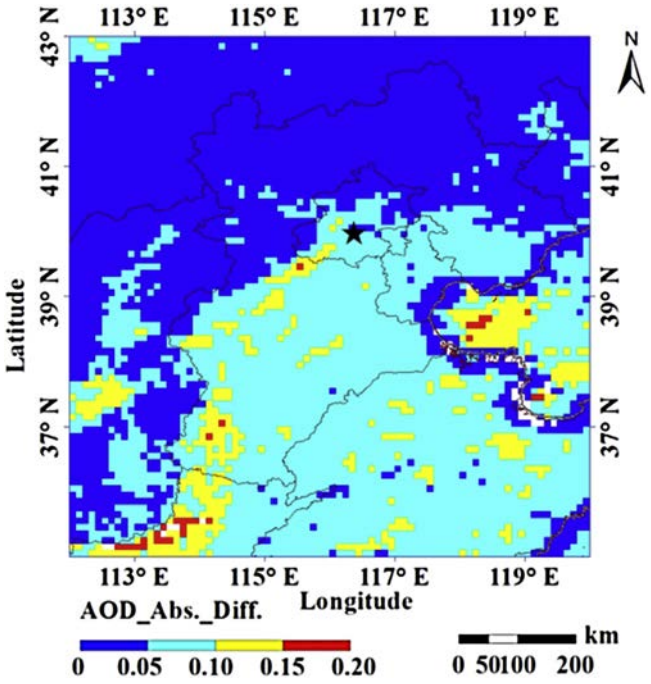

Fig. 1. The spatial distribution of AOD differences between MODIS/Terra AOD and MODIS/Aqua AOD during the period from January to December 2010. The star represents Beijing AERONET station.

2.1.1. AERONET data

In the present study, ground-based AODs were measured using a CIMEL 318 radiometer. This instrument is available at the AERONET stations, which form a global network of sun photometers. AERONET data are used to derive AOD and other aerosol characteristics using an inversion method applied to measurements of downwelling solar radiation (Holben et al., 1998; Dubovik and King, 2000). Standard protocol makes that AOD is provided every 15 min for spectral bands centered at 340, 380, 440, 500, 675, 870, and 1020 nm with an accuracy of ±0.02. For the level 2.0 products, the AOD uncertainties are of the order of 0.01 in the visible and near-infrared channels (Eck et al., 1999). In this study, instantaneous AOD data at 440 nm and Ångström exponent within 440−675 nm are retrieved from the cloud screened and quality-assured Level 2.0 of AERONET. AOD estimates derived from AERONET are converted to 550 nm using the Ångström coefficient within 440−675 nm (e.g. Ångström, 1929). In this research we analyzed radiometer data from January to December 2010.

2.1.2. MODIS data

The MODIS instrument, aboard the pair of low Earth orbit (LEO) satellites Terra and Aqua, observes the Earth with a total swath of more than 2300 km and a revisit cycle of one to two days. MODIS measures the TOA radiance with 36 spectral bands from 0.4 to

14.2 μm (Salomonson et al., 1989). In this study, the Collection 6 Level 2 MOD04 and MYD04 aerosol products (Levy et al., 2013) are considered. Instantaneous AOD values at 550 nm corresponding to the aerosol conditions at the time of the overpass of the Terra and Aqua satellites are disseminated with a spatial resolution of 10 km. For each collocated MODIS- and AERONET-observed AOD data pair, the average MODIS AOD over 3 × 3 MODIS grids centered at Beijing AERONET site has to be determined. Meanwhile, the hourly average AOD at Beijing AERONET site is calculated from the observations taken within ±30 min of the MODIS overpasses. Here we analyzed radiometric data from the whole year 2010.

2.1.3. Surface albedo data

In this paper, we use the daily-averaged surface albedo (α), which is borrowed from the climatology constructed using seven years (2004–2010) of MODIS black-sky visible albedo. In particular, we use the MCD43 product from collection 5.0, which is obtained by inverting multi-date, multi-angular, cloud-free, atmospherically corrected, surface reflectance observations acquired by the MODIS instruments on board the Terra and the Aqua satellites over a 16-day period. The accuracy of the high quality MODIS operational albedo is well less than 5% at the majority of the validation sites studied by Cescatti et al. (2012). In addition, only albedo values with a high confidence index were used to build the albedo climatology used in the present article. The latter was built at a spatial resolution of 0.05° × 0.05°. Black-sky albedo was preferred to white-sky or blue sky-albedos because it is not impacted by aerosols and therefore allows us to consider only the radiative effect arising from the intrinsic surface properties.

2.2. Methodology

2.2.1. Aerosol radiative forcing calculations

Generally speaking, the clear-sky DARF (ΔF; Wm^{-2}) is defined as the difference between the net flux with aerosol and the net flux without aerosol, which can be expressed as:

$$\Delta F_i = F_{net,i} - F'_{net,i} \tag{1}$$

where i may represent "at the top of atmosphere (TOA)" or "at the surface (SUR)", $F_{net,i}$ represents the net flux with aerosol, and $F'_{net,i}$ represents the net flux without aerosol.

$F_{net,i}$ can be calculated as the difference between the downwelling flux with aerosol ($F_{\downarrow,i}$) and upwelling flux with aerosol ($F_{\uparrow,i}$), given as below:

$$F_{net,i} = F_{\downarrow,i} - F_{\uparrow,i} \tag{2}$$

Similarly, F'_{net} denotes the difference between the downwelling flux without aerosol ($F'_{\downarrow,i}$) and the upwelling flux with aerosol ($F'_{\uparrow,i}$), which is formulated as follows:

$$F'_{net,i} = F'_{\downarrow,i} - F'_{\uparrow,i} \tag{3}$$

Combining Eqs. (1)–(3), we obtain the following expression:

$$\Delta F_i = \left(F_{\downarrow,i} - F_{\uparrow,i}\right) - \left(F'_{\downarrow,i} - F'_{\uparrow,i}\right) \tag{4}$$

Since the downward flux at the top of the atmosphere is independent of the presence of aerosols (i.e., $F_{\downarrow,TOA} = F'_{\downarrow,TOA}$), the clear-sky DARF at TOA (ΔF_{TOA}) is derived as follows:

$$\Delta F_{TOA} = F'_{\uparrow,TOA} - F'_{\uparrow,TOA} \tag{5}$$

On the other hand, the upward flux at the surface ($F_{\uparrow,SUR}$) can be estimated in terms of the downward flux and the α such as

$$F_{\uparrow,SUR} = \alpha F_{\downarrow,SUR} \tag{6}$$

If i in Eq. (4) is replaced with SUR, we get the DARF at the surface (ΔF_{SUR}) as:

$$\Delta F_{SUR} = \left(F_{\downarrow,SUR} - \alpha F_{\downarrow,SUR}\right) - \left(F'_{\downarrow,SUR} - \alpha F'_{\downarrow,SUR}\right) \tag{7}$$

which can be further written as:

$$\Delta F_{SUR} = (1-\alpha)\left(F_{\downarrow,SUR} - F'_{\downarrow,SUR}\right) \tag{8}$$

The DARF in the atmosphere (ΔF_{ATM}) is defined as:

$$\Delta F_{ATM} = \Delta F_{TOA} - \Delta F_{SUR} \tag{9}$$

The daily mean $\overline{\Delta F}$ is given by (Min and Zhang, 2013):

$$\overline{\Delta F} = \frac{1}{T_{day}} \int_{T_{sunrise}}^{T_{sunset}} \Delta F\left[\theta^0(t), \tau(t)\right] dt \tag{10}$$

where T_{day} is the total number of hours in a day depending on the difference between T_{sunset} and $T_{sunrise}$; $T_{sunrise}$ and T_{sunset} are the sunrise and sunset time; θ^0 is solar zenith angle and τ stands for AOD here.

2.2.2. Radiative transfer calculations

For the simulations of downward flux reaching the Earth's surface ($F_{\downarrow,SUR}$ and $F'_{\downarrow,SUR}$) and upward flux reaching the top of the atmosphere ($F_{\downarrow,TOA}$ and $F'_{\downarrow,TOA}$), we employed the radiative transfer model 6S (Second Simulation of a Satellite Signal in the Solar Spectrum) (Vermote et al., 1997), which is widely used to simulate the signals observed by a satellite sensor transmitted through a coupled surface-atmosphere medium for a broad range of spectral, geometrical and atmospheric situations (Kotchenova et al., 2006). A cloudless U.S. 62 standard atmosphere is chosen to set typical content and vertical profiles for atmospheric gases. The aerosol model chosen for Beijing site is continental. For ground reflectance, we consider a homogeneous and Lambertian surface with seasonal mean surface albedo averaged from the albedo climatology presented in Section 2.1.3. In order to estimate the influence of AOD diurnal variation on the DARF calculations using MODIS data, seasonally averaged hourly AERONET AOD values are used as input. In addition, both Terra and Aqua AOD are also used as input. Using the 1-h time step, we performed the 6S calculations during a daytime with the solar zenith angle corresponding to April 15th, July 15th, October 15th, January 15th to get the seasonal DARF results of spring, summer, autumn and winter, respectively. Similarly, we chose June 30th in order to get the annual results.

Estimation of DARF strongly depends on the aerosol type and the albedo of the underlying surface (Keil and Haywood, 2003). Therefore, sensitivity study is performed by running 6S for different aerosol types such as dust, continental, biomass burning aerosols and for different surface albedo values ($0.1 \leqq \alpha \leqq 0.9$) to compute the diurnal variation of DARF and the daily averaged DARF using hourly averaged AODs during the daytime. Here, AOD diurnal cycle during summertime is used.

3. Results and discussion

3.1. Diurnal variations of AOD

The diurnal variations of hourly averaged AERONET-observed AOD at 550 nm in Beijing site for spring, summer, autumn, winter, and the whole year of 2010 are present in Fig. 2. The vertical

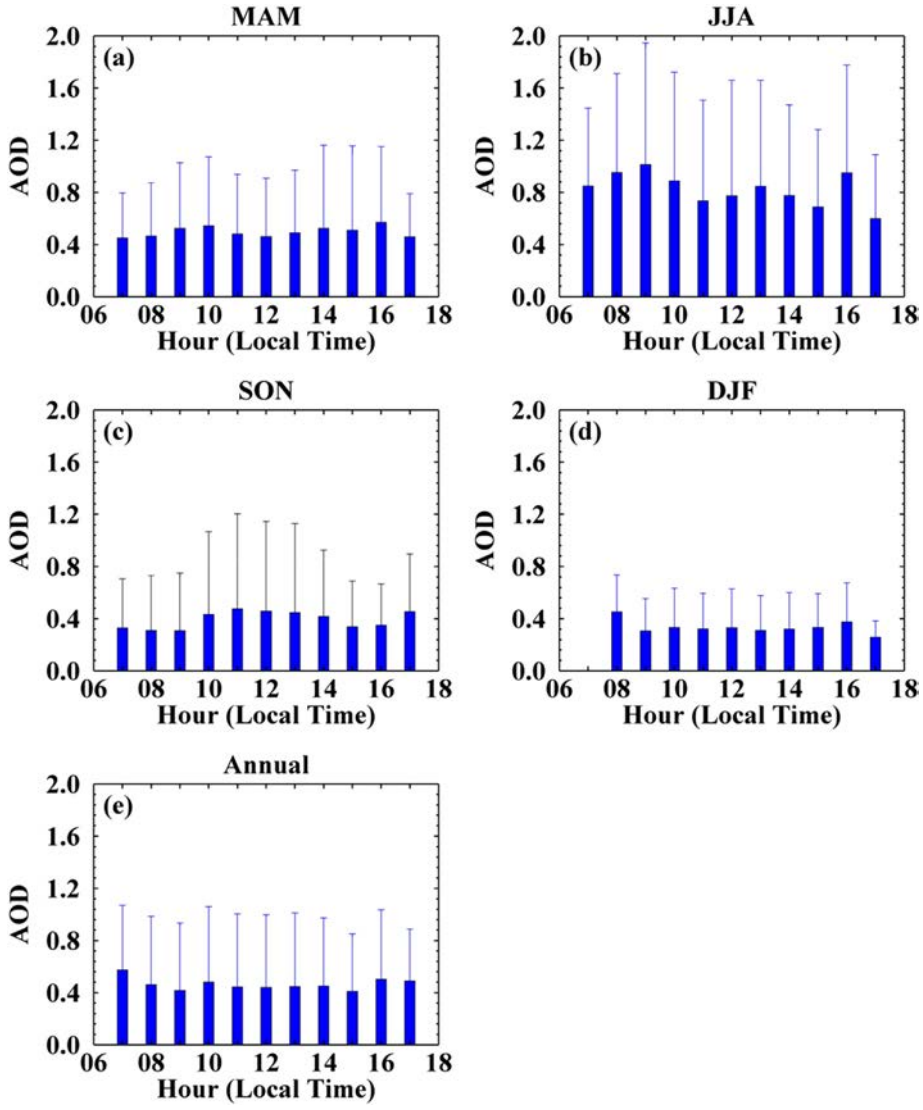

Fig. 2. Diurnal cycle (0700 LT to 1700 LT) of hourly averaged AERONET AOD at 550 nm in (a) spring (MAM), (b) summer (JJA), (c) autumn (SON), (d) winter (DJF) of the year 2010, and (e) during the all months of January through December of 2010 at Beijing site. Note that the error bars represent one standard deviation.

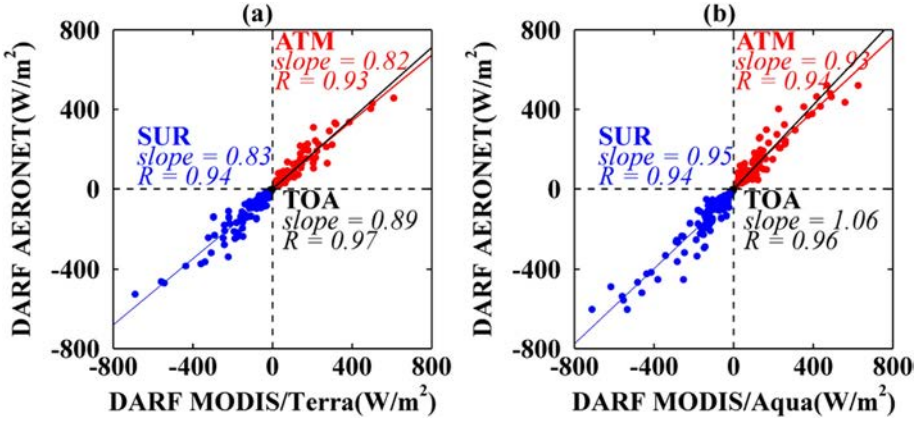

Fig. 3. Scatterplots of the instantaneous DARFs (Wm-2) in the atmosphere (ATM, in red), at the top of atmosphere (TOA, in black) and at the surface (SUR, in blue) as calculated from (a) MODIS/Terra AOD, (b) MODIS/Aqua AOD versus coincident AERONET AOD at Beijing site. The regression lines of MODIS DARFs against AERONET DARFs are given as well. Note that all samples are limited to the period from January to December 2010. (For interpretation of the references to colour in this figure legend, the reader is referred to the web version of this article.)

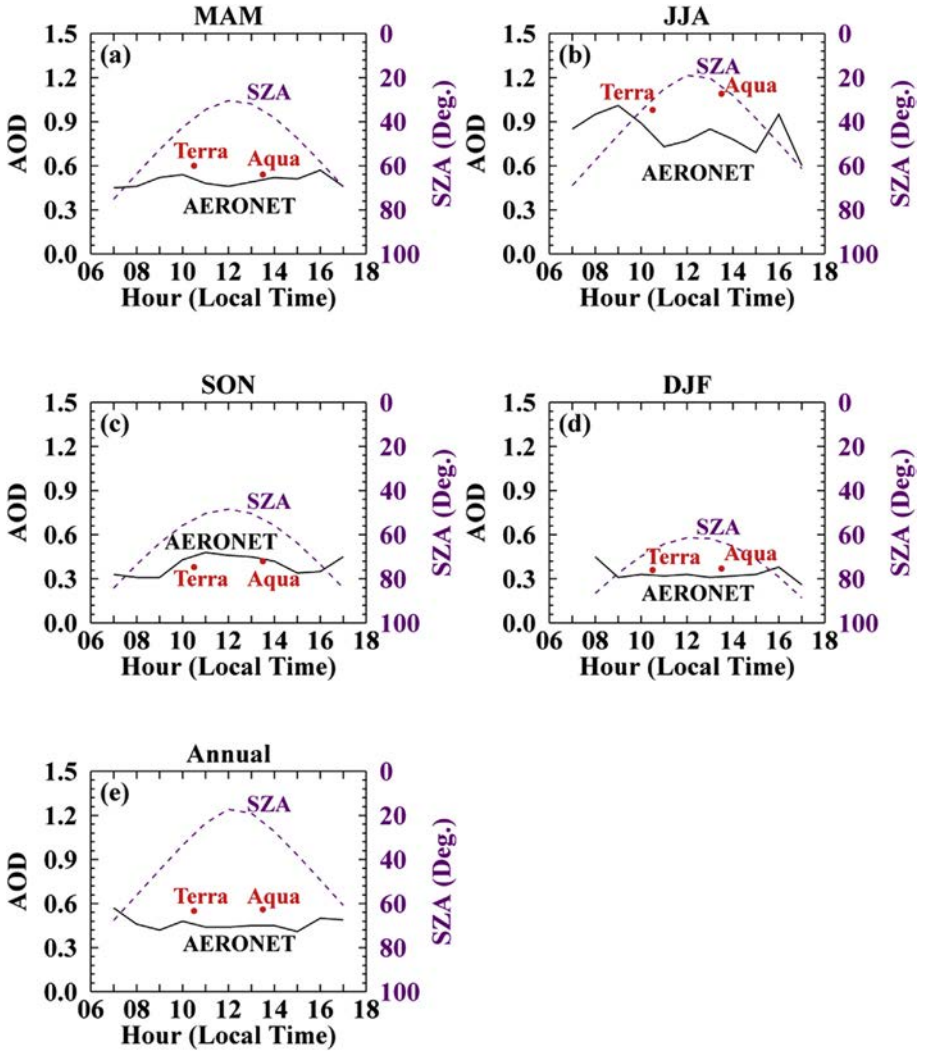

Fig. 4. The diurnal variations of hourly averaged AERONET-observed AOD values (in black curves) at Beijing site in (a) spring, (b) summer, (c) autumn, (d) winter, and (e) the whole year of 2010. The red solid circles correspond to daily mean MODIS/Terra and MODIS/Aqua AOD. The purple curves represent diurnal variation of solar zenith angle. (For interpretation of the references to colour in this figure legend, the reader is referred to the web version of this article.)

bars over the data points of each hour represent the standard deviation of the AOD. Only the local time (LT) range from 0700 to 1700 is considered, since the direct interaction of aerosol with the solar radiation only happens during daytime. The annual daily averaged AOD at Beijing is 0.46, which means that the Beijing city is highly polluted. The seasonal daily averaged AOD presents some peaks in spring (0.49) and summer (0.81) and the lowest values in autumn (0.39) and winter (0.30). Gong et al. (2014) also reported a similar value of seasonal mean AOD in Beijing, which is higher in spring and summer and lower in autumn and winter. Seasonal daily averaged AOD values are relatively high in spring due to the occasional long-range transportation of dust aerosols upwind from dust source regions. The highest AOD in summer is associated with increased human activities, such as biomass burning, as well as the hygroscopic growth of aerosols due to enhanced relative humidity (Wu et al., 2015).

The observed AOD showed an appreciable diurnal variability. Difference between the maximum and minimum values varies from 0.12 to 0.41 depending on the seasons. In summer and spring, the diurnal values of AOD are higher between 0800 LT and 1000 LT in the morning and 1600 LT in the afternoon. During spring, the diurnal changes of AOD are small ranging from −8 to 16% on AOD as shown in Fig. 2a. The daily averaged AOD value in spring is 0.49 with a maximum 0.57 and a minimum 0.45. During summer, the diurnal changes of AOD are large ranging from −26 to 25% on AOD (Fig. 2b). The daily averaged AOD value in summer is 0.81 with a maximum 1.01 and a minimum 0.60. This result is similar to some previous studies on the diurnal variation of AOD (Wang et al., 2015a, b; Kuang et al., 2015). In autumn, the value of AOD is higher between 1000 LT and 1400 LT at noon and at 1600 LT in the evening. During autumn, the diurnal changes of AOD are moderate ranging from −21 to 23% on AOD (Fig. 2c). The daily averaged AOD value in autumn is 0.39 with a maximum 0.48 and a minimum 0.31. In winter, AOD also exhibits moderate diurnal variation, which ranges from −21 to 36% on AOD (Fig. 2d). The averaged AOD value is 0.33 with a maximum 0.45 and a minimum 0.26, and generally reaches the peak at 0800 LTand 1600 LT.

3.2. Comparison between instantaneous DARFs estimated by MODIS-derived and AERONET-observed AOD

To confirm the reliability of the DARF calculated by the MODIS-derived AOD, the instantaneous DARF calculated by the AOD derived from MODIS/Terra and MODIS/Aqua versus that observed

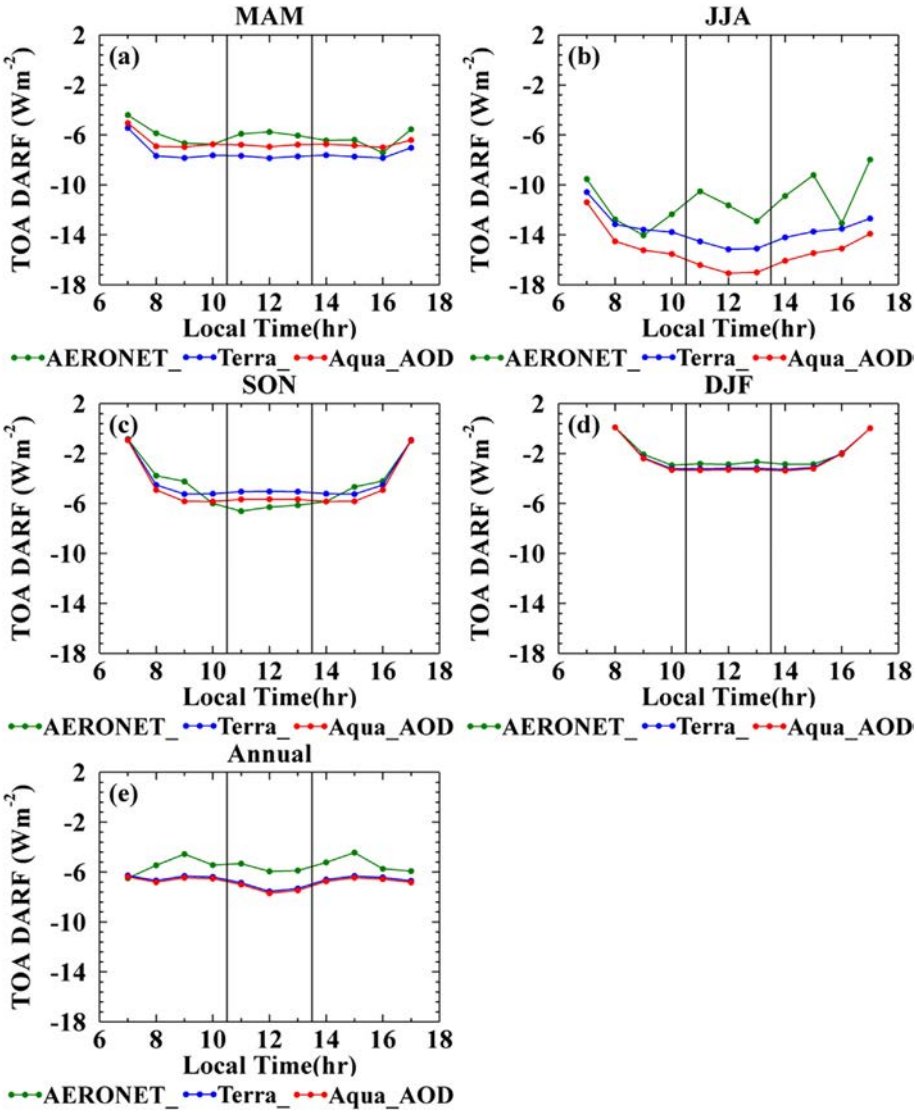

Fig. 5. Diurnal variations of clear-sky DARFs at TOA in spring (a), summer (b), autumn (c), winter (d), and the whole year (e), which take the following three AODs as inputs into radiative transfer models: 1. hourly averaged AERONET-observed AOD in Fig. 3 (green solid circles); 2. constant MODIS/Terra AOD (blue solid circles); 3. constant MODIS/Aqua AOD (red solid circles). The vertical lines correspond to Terra and Aqua crossing times. (For interpretation of the references to colour in this figure legend, the reader is referred to the web version of this article.)

from AERONET are compared in Fig. 3. In general, the DARF at TOA and SUR are negative, whereas the DARF in ATM (energy absorbed in the aerosol layer) is positive. The correlation coefficients of DARF estimates calculated by MODIS/Terra AOD and AERONET-observed AOD are 0.93 in ATM, 0.94 at TOA and 0.97 at SUR, respectively as shown in Fig. 3a. Similarly, the DARF calculated by the MODIS/Aqua AOD compares well with that by AERONET-observed AOD as shown in Fig. 3b. The correlation coefficients of these two DARFs can reach to 0.93 in ATM, 0.94 at TOA, and 0.96 at SUR, respectively. These results show that instantaneous DARF estimated by MODIS/terra and MODIS/Aqua AOD are both in good agreement with that calculated by AERONET observed AOD. This good relationship between MODIS and AERONET derived instantaneous DARF revealed that the MODIS-derived AOD could be used to estimate the DARF.

It is interesting to note that the slopes of DARF estimates calculated by MODIS/Terra AOD and AERONET-observed AOD are only 0.82 in ATM, 0.89 at TOA, and 0.83 at SUR, which are less than that of MODIS/Aqua AOD with the slopes are 0.93 in ATM, 1.06 at TOA and 0.95 at SUR, respectively. This result is not consistent with previous studies which demonstrate that there is no significant difference between the uncertainties in MODIS/Terra and MODIS/Aqua AOD (Remer et al., 2005; Levy et al., 2007). The reason may be that MODIS/Terra AOD is decreasing, whereas MODIS/Aqua is increasing over time (Levy et al., 2010).

3.3. *Influence of AOD diurnal cycle on clear-sky DARF*

The averaged MODIS-derived (including Terra and Aqua) AOD values and diurnal variations of hourly averaged AOD values observed by AERONET for spring, summer, autumn, winter and the whole year of 2010 are superimposed in Fig. 4. The diurnal cycles of solar zenith angle at the Beijing site on Jan. 15th, Apr. 15th, Jul. 15th, Nov. 15th and Jun. 30th 2010 are plotted in Fig. 4 as well. The five plots correspond to spring, summer, autumn, winter and year-round averages, respectively.

The diurnal variations of DARF at TOA calculated using constant MODIS-derived AOD (including Terra and Aqua) during the daytime for each season and the year-round are shown in Fig. 5. The

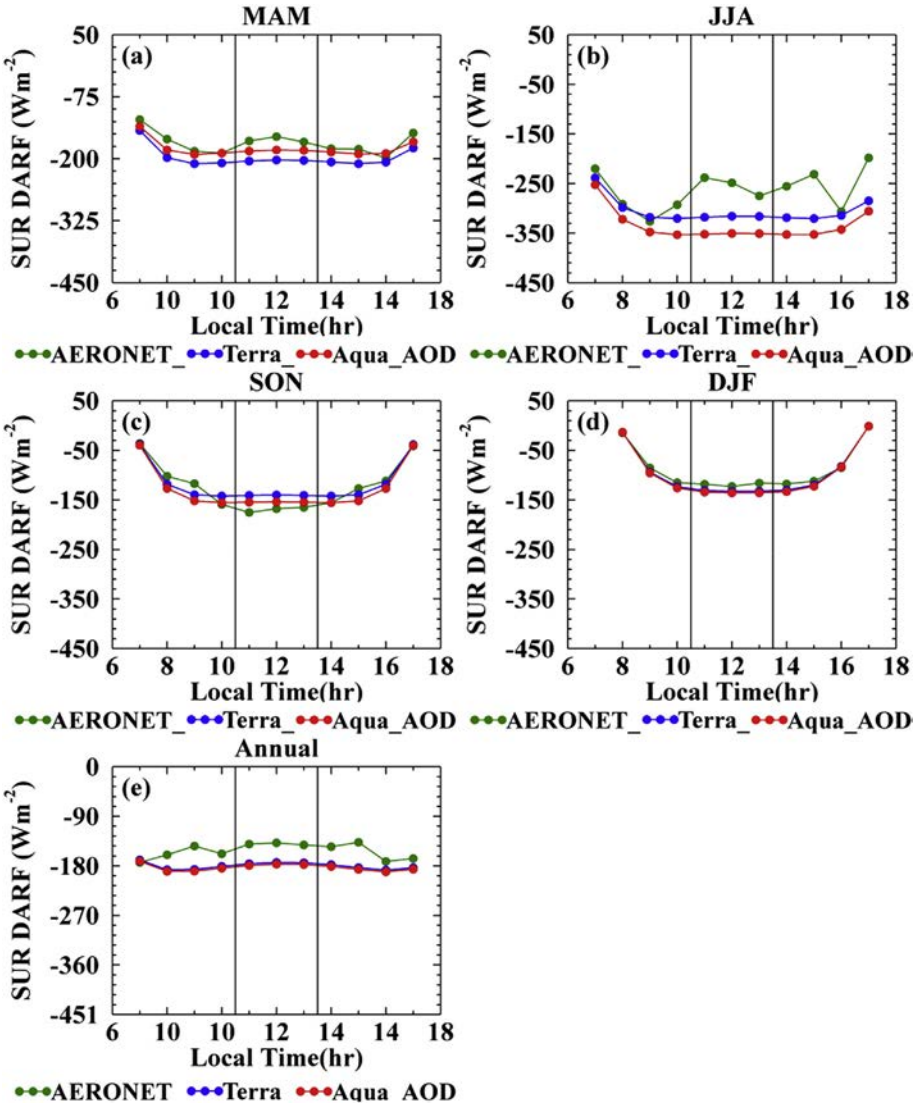

Fig. 6. Diurnal variations of clear-sky DARFs at SUR in spring (a), summer (b), autumn (c), winter (d), and the whole year (e), which take the following AODs as inputs into radiative transfer models: 1. hourly averaged AERONET-observed AOD in Fig. 3 (green solid circles); 2. constant MODIS/Terra AOD (blue solid circles); 3. constant MODIS/Aqua AOD (red solid circles). The vertical lines correspond to Terra and Aqua crossing times. (For interpretation of the references to colour in this figure legend, the reader is referred to the web version of this article.)

seasonal and annual means of DARF at TOA are negative throughout the year of 2010 in Beijing City. The reason to this may be that the dominant aerosols in the metropolitan area are scattering aerosols which typically exert a negative DARF (Gong et al., 2014). In order to quantify the impact of AOD diurnal variation on the estimation of daily averaged DARF at TOA using MODIS-derived AOD, the diurnal variations of DARF at TOA calculated using hourly averaged AERONET-observed AOD are shown in Fig. 5 as well. It can be seen that the diurnal variation of the DARF at TOA calculated using hourly AOD variability is dependent on both the variation of solar zenith angle and the AOD diurnal cycle. Similar to the case of AOD diurnal variations (see Fig. 2), largest diurnal variations were observed in the DARF in ATM, at TOA and SUR, during summertime. This means, if the constant MODIS-derived AOD value is used instead of the true AOD variability, it might result in a large bias in the estimation of daily average DARF at TOA and SUR when the diurnal variation of AOD is significant. This result is consistent with the research of Arola et al. (2013), which demonstrate that, for individual site; there can be significant biases in the estimates of DARF due to the diurnal AOD variability. Using constant MODIS/Terra or MODIS/Aqua AOD value generally leads to overestimating of the negative daily averaged DARF at TOA, due to the overestimation of MODIS-derived AOD. Because the dominant aerosols in Beijing are scattering aerosols, a larger AOD will cause more scattering of incident solar radiation by atmospheric aerosol, more light reflected into space, and thus a larger negative DARF at TOA. Similar to DARF at TOA, daily averaged DARF at SUR is also overestimated by using constant MODIS-derived AOD value instead of AOD variability (Fig. 6). The reason maybe that the overestimation of scattering aerosols will therefore result in less light reaching the surface, and thus a larger negative DARF at SUR. In contrast to the case of DARF at TOA and SUR, due to the AOD cycle, daily averaged DARF in ATM is always underestimated by using constant MODIS-derived AOD value (Fig. 7).

The diurnal cycle of AOD cannot be captured by using MODIS/Terra or MODIS/Aqua data alone, because only one AOD estimate is available per day at most. Therefore, differences in daily averaged DARF in ATM, at TOA and SUR for each season and the year-round

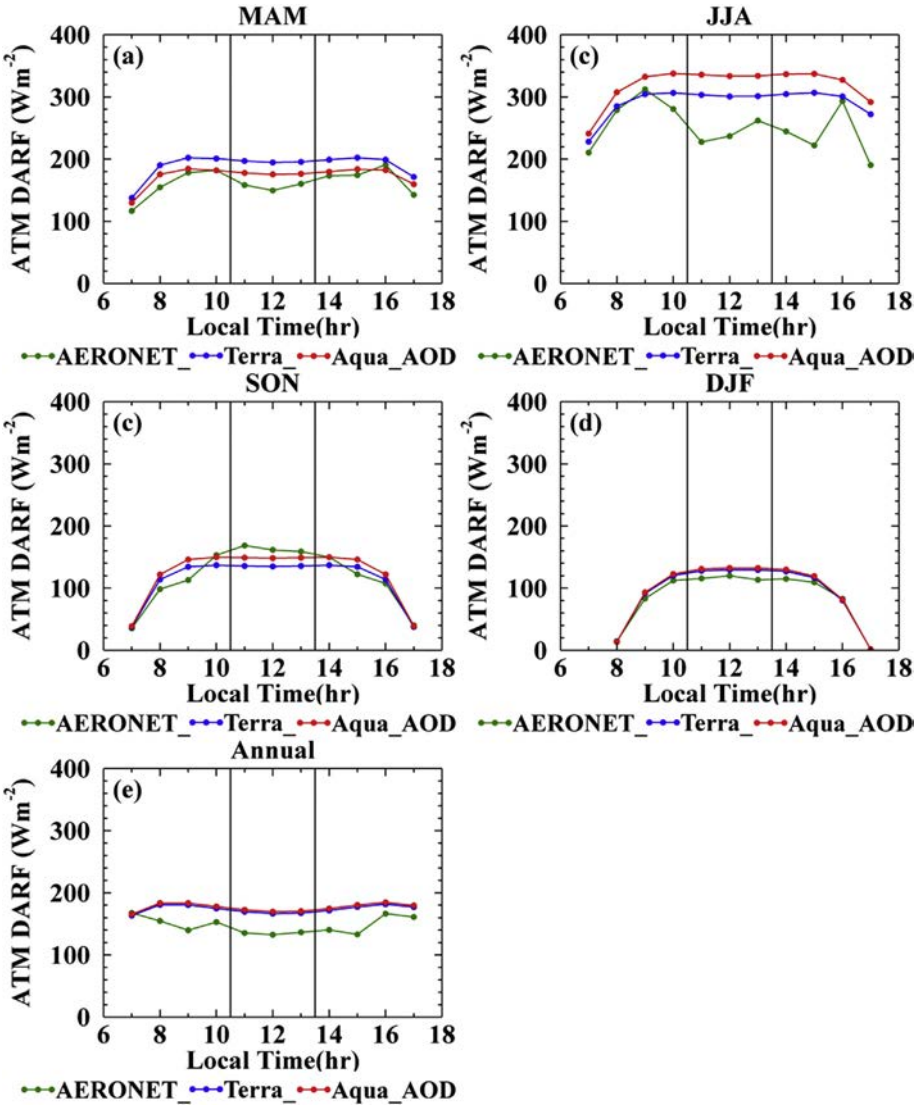

Fig. 7. Diurnal variations of clear-sky DARFs in ATM in spring (a), summer (b), autumn (c), winter (d), and the whole year (e), which take the following AODs as inputs into radiative transfer models: 1. hourly averaged AERONET-observed AOD in Fig. 3 (green solid circles); 2. constant MODIS/Terra AOD (blue solid circles); 3. constant MODIS/Aqua AOD (red solid circles). The vertical lines correspond to Terra and Aqua crossing times. (For interpretation of the references to colour in this figure legend, the reader is referred to the web version of this article.)

are shown in Fig. 8, when the constant MODIS/Terra or MODIS/Aqua AOD value is used instead of AERONET-observed AOD variability. If constant MODIS/Terra or MODIS/Aqua AOD is used, the daily averaged DARF at TOA is absolutely overestimated by the range of 0.2–3.9 Wm^{-2} (4.4–34.2% in relative ones) with 2.0 Wm^{-2} on average for each season and by around 1.2 Wm^{-2} for the year-round (Fig. 8a). It is interesting to note that the AOD diurnal variation in spring is small than in autumn, but the difference in DARF at TOA in spring is larger than that in autumn. The reason may be that the maximum AOD occurred around Terra overpass time. This results indicating that larger bias may exist in the estimation of daily averaged even if the AOD diurnal variation is small. Similar scientific findings have been offered in previous literature (e.g., Kassianov et al., 2013), which demonstrated that the bias in the 24-h average DARF estimations due to a limited diurnal coverage of AOD (only morning or evening observations available) could be as large as 100%. Similarly, the diurnal AOD cycle induces a variation between the DARF at SUR calculated by AERONET-observed AOD variability and the constant MODIS-derived AOD from 4.9 to 72.7 Wm^{-2} in absolute values with 38.8 Wm^{-2} on average for each season and by around 29.0 Wm^{-2} for annual (Fig. 8b). In ATM, the bias caused by using constant MODIS-derived AOD varies from to 4.7 to 68.8 Wm^{-2} with 36.8 Wm^{-2} on average for each season and by around 28.0 Wm^{-2} for annual (Fig. 8c). These result indicating that AOD diurnal variations play a significant role in the estimation of DARFs. Consequently, the influence of diurnal AOD variability on the estimates of daily average DARF at TOA using MODIS-derived AOD cannot be ignored.

3.4. Sensitivity of MODIS-derived DARF to surface albedo and aerosol types

Previous studies suggested that DARFs are sensitive to the albedo of the underlying surface (Seinfeld, 2008; Chylek et al., 1974; Ma and Yu, 2012). Brighter surfaces reflect more solar radiation to the atmosphere and thus lead to more re-absorption and re-scattering of solar radiation by aerosols (Zhuang et al., 2014). To quantify the effects of surface albedo on the estimation of DARF

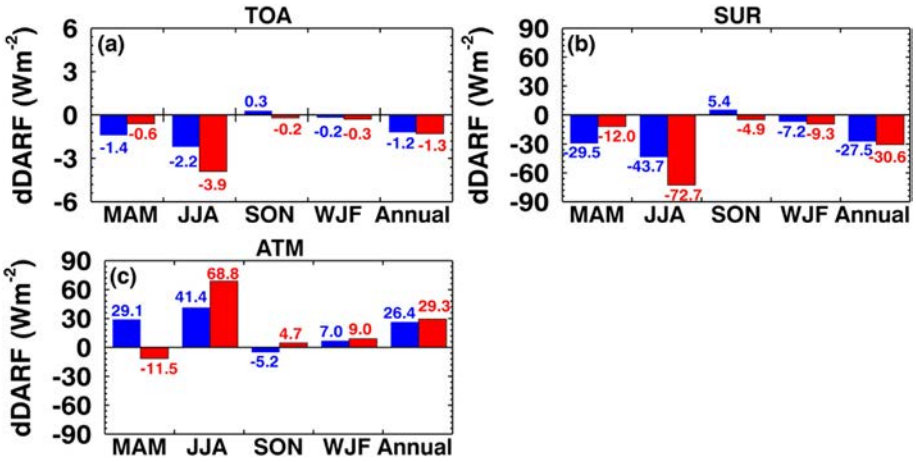

Fig. 8. Histograms of seasonal and annual differences in daily averaged DARFs at TOA (a), at SUR (b), and in ATM (c). Blue (Red) bar is the difference in daily averaged DARFs between hourly averaged AERONET and observed AOD throughout the daytime and constant MODIS/Terra (MODIS/Aqua) AOD. (For interpretation of the references to colour in this figure legend, the reader is referred to the web version of this article.)

using MODIS-derived AOD over Beijing, sensitivity tests were carried out as described in Section 2.2.2. Using constant MODIS-derived AOD during the daytime, the daily averaged DARFs in ATM, at TOA and SUR during summertime under different surface albedos are calculated as shown in Fig. 9. At TOA, estimated DARF using constant MODIS/Terra or MODIS/Aqua AOD is negative over dark surface ($\alpha < 0.2$) and positive over bright surface ($\alpha > 0.2$). The reason for this may be due to that less radiation is scattered by scattering aerosols in Earth-atmosphere system with brighter surfaces. A similar conclusion is reached from previous study (Zhuang et al., 2014). Changes in DARF at SUR are different, as it becomes less negative with increasing surface albedo. Finally, DARF in ATM decreases with increasing surface albedo. These results indicate that the MODIS-derived DARF is sensitive to surface albedo.

In order to study the impact of different albedos on the estimation of DARF using MODIS-derived AOD, the daily averaged DARFs in ATM, at TOA and SUR in summer under different surface albedos, calculated by hourly averaged AERONET–observed AODs during the daytime, are shown in Fig. 9 as well. Fig. 9a shows that the bias in the estimated DARF at TOA caused by using constant MODIS-derived AOD is lowest for a relatively dark surface (surface albedo of 0.2). When the surface albedo is lower (larger) than 0.2, the bias decreases (increases) for a higher surface albedo. Due to AOD variability, the bias in the estimated DARF at SUR (in ATM)

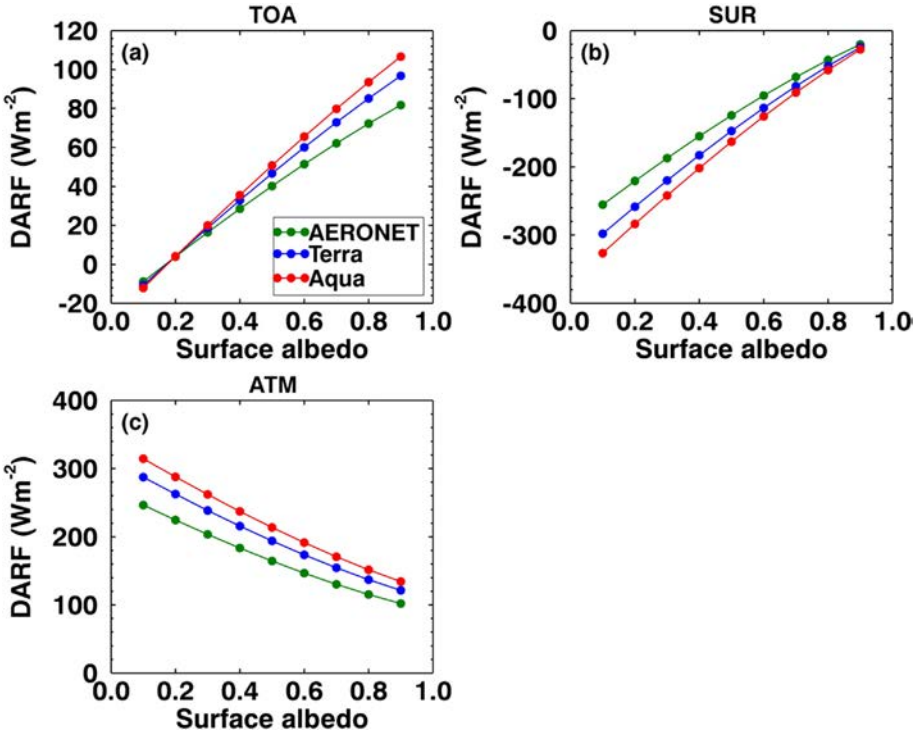

Fig. 9. Simulated daily averaged DARFs at TOA (a), at SUR (b), and in ATM (c) during the summertime based on the assumptions of various surface albedo, which take the following AODs as inputs into radiative transfer models: 1. hourly averaged AERONET-observed AOD in Fig. 3 (green solid circles); 2. constant MODIS/Terra AOD (blue solid circles); 3. constant MODIS/Aqua AOD (red solid circles). (For interpretation of the references to colour in this figure legend, the reader is referred to the web version of this article.)

Table 1
Summaries of daily averaged DARFs (Wm^{-2}) at TOA (ΔF_{TOA}) and SUR (ΔF_{SUR}), in ATM (ΔF_{ATM}) in summer for aerosol types such as dust, continental and biomass burning under different surface albedos ($\alpha = 0.1$, 0.2 and 0.3), as calculated from hourly averaged AERONET AODs throughout the daytime (τ), MODIS/Terra AOD (τ_{Terra}), and MODIS/Aqua AOD (τ_{Aqua}). Their corresponding differences in DARFs and their percentages are given as well.

Aerosol types	Surface albedos	τ	τ_{Terra}	τ_{Terra}-τ	τ_{Aqua}	τ_{Aqua}-τ
Dust	$\alpha = 0.1$	−17.2	−20.0	−2.8 (16.3%)	−23.6	−6.4 (37.2%)
	$\alpha = 0.2$	−8.5	−10.7	−2.2 (25.9%)	−12.4	−3.9 (45.9%)
	$\alpha = 0.3$	−0.6	−1.3	−0.7 (117.6%)	−2.0	−1.4 (233.4%)
Biomass burning	$\alpha = 0.1$	−14.9	−18.3	−3.4 (22.8%)	−20.6	−5.7 (38.3%)
	$\alpha = 0.2$	−3.7	−5.1	−1.4 (37.8%)	−6.2	−2.5 (67.6%)
	$\alpha = 0.3$	7.0	7.5	0.5 (7.1%)	7.7	0.7 (10.0%)
Continental	$\alpha = 0.1$	−8.9	−10.7	−1.8 (20.2%)	−12.1	−3.2 (36.0%)
	$\alpha = 0.2$	3.9	4.1	0.2 (5.1%)	4.0	0.1 (2.6%)
	$\alpha = 0.3$	16.4	18.6	2.2 (13.4%)	20.0	3.6 (22.0%)

caused by using constant MODIS-derived AOD is lower over bright surfaces than over dark surfaces, due to the less negative (positive) DARF at SUR (in ATM).

Except surface albedo, aerosol type is also important for the estimation of DARF, especially at the top of the atmosphere. Whether aerosols exert a net cooling or a warming effect will depend on the aerosol type and the albedo (Chand et al., 2009; Keil and Haywood et al., 2003). In order to quantify the impact of different aerosol types on the estimation of DARF, sensitivity tests are carried out as described in Section 2.2.2. Table 1 show the daily averaged DARFs at TOA, as well as the influence of AOD diurnal cycle on DARF in summer for different aerosol types such as dust, continental, and biomass burning aerosols under different surface albedos ($\alpha = 0.1$, 0.2 and 0.3). For dust aerosols, the surface albedo at which DARFs at TOA change from negative to positive is larger than 0.3. As for continental aerosols, it is a totally different story. The reason may be related to the difference in the scattering properties of these two aerosol types. In general, DARFs at TOA are negative over dark surface ($\alpha = 0.1$) for dust, continental and biomass burning aerosols, indicating these aerosols have a cooling effect on Earth system. This result is consistent with previous study (Yu et al., 2006). The diurnal AOD cycle cannot be captured by means of MODIS AOD data, which makes us choose AERONET AOD to estimate DARF and thus assess their differences. It can be clearly seen that, for negative DARFs, the higher the surface albedo, the stronger impact on estimates of DARFs at TOA. For dust aerosols, the impact on estimates of DARFs using constant MODIS/Terra (MODIS/Aqua) data estimates can reach up to 117.6% (233.4%). The magnitude of influence becomes 37.8% (67.6%) for biomass burning aerosols. However, for continental aerosols, the impact on estimates of DARFs using constant MODIS/Terra (MODIS/Aqua) data estimates is less than 20.2% (36.0%). Interestingly, the biases in the calculation of DARF at TOA caused by using MODIS/Aqua AOD seems systematically to be larger compared with using MODIS/Terra AOD. The underlying factors leading to this difference warrant a further investigation in the future.

4. Summary

In this study the influence of the diurnal variation in AOD on the MODIS (aboard Terra and Aqua) - derived DARFs at the top of the atmosphere, surface and in the atmosphere has been investigated at the AERONET Beijing site, China, during the year of 2010. To perform such an investigation, we calculated seasonal and annual mean of the hourly averaged AERONET observed AOD data as input for the radiative transfer code 6S, and compared them to the daily averaged DARF calculated using single MODIS Terra and Aqua AOD values as inputs.

Assuming constant MODIS/Terra (MODIS/Aqua) AOD throughout the daytime instead of the observed diurnal variation of AOD in determining daily averaged DARF, we found that the daily averaged DARF estimates is on average underestimated by around 2.0 Wm^{-2} at TOA and around 38.8 Wm^{-2} at SUR. By contrast, it is overestimated by around 36.8 Wm^{-2} in terms of DARF in ATM. The impact on DARF estimates using MODIS-derived AOD data not only depend on the diurnal variation of AOD during the daytime but also depend on whether the maximum AOD occurred around the Terra or Aqua overpass time.

The impact of using MODIS-derived AOD for estimation of DARF at TOA is sensitive to surface albedo and aerosol type. For negative DARFs, the impact on estimates of DARFs at TOA using constant MODIS AOD data grows with the increase in surface albedo. For different aerosol types, DARF estimates at TOA changes from negative to positive, depending on the surface albedo. For dust aerosols, the impact on estimates of DARFs using constant MODIS/Terra (MODIS/Aqua) data estimates can reach up to as large as 117.6% (233.4%). Therefore, special care must be taken when aiming to obtain accurate DARF calculations at TOA for dust and biomass burning aerosols over dark surface ($\alpha = 0.2$) based on MODIS data alone.

Acknowledgements

The work was performed under the auspices of Ministry of Science and Technology of the People's Republic of China (Grant 2014BAC16B01), Natural Science Foundation of China (Grants 41590874, 91544217, 41471301, 41405035,) and Chinese Academy of Meteorological Sciences (Grant 2014R18), Guangdong Provincial Science and Technology Plan Projects (Grant 2014A010101151). The MODIS AOD data used in this study were also acquired as part of the NASA's Earth-Sun System Division and archived and distributed by the Goddard Earth Sciences (GES) Data and Information Services Center (DISC) Distributed Active Archive Center (DAAC).

References

Adhikary, B., Kulkarni, S., Dallura, A., Tang, Y., Chai, T., Leung, L.R., Qian, Y., Chung, C.E., Ramanathan, V., Carmichael, G.R., 2008. A regional scale chemical transport modeling of Asian aerosols with data assimilation of AOD observations using optimal interpolation technique. Atmos. Environ. 42 (37), 8600–8615. http://dx.doi.org/10.1016/j.atmosenv.2008.08.031.

Arola, A., Eck, T.F., Huttunen, J., Lehtinen, K.E.J., Lindfors, A.V., Myhre, G., Smirnov, A., Tripathi, S.N., Yu, H., 2013. Influence of observed diurnal cycles of aerosol optical depth on aerosol direct radiative effect. Atmos. Chem. Phys. 13, 7895–7901. http://dx.doi.org/10.5194/acp-13-7895-2013.

Ångström, A., 1929. On the atmospheric transmission of sun radiation and on dust in the air. Geogr. Ann. 11, 156–166. http://dx.doi.org/10.2307/519399.

Cescatti, A., Marcolla, B., Santhana Vannan, S.K., Pan, J.Y., Román, M.O., Yang, X., Ciais, P., Cook, R.B., Law, B.E., Matteucci, G., Migliavacca, M., Moors, E., Richardson, A.D., Seufert, G., Schaaf, C.B., 2012. Intercomparison of MODIS albedo retrievals and in situ measurements across the global FLUXNET network. Remote Sens. Environ. 121, 323–334. http://dx.doi.org/10.1016/j.rse.2012.02.019.

Chand, D., Wood, R., Anderson, T.L., Satheesh, S.K., Charlson, R.J., 2009. Satellite-

derived direct radiative effect of aerosols dependent on cloud cover. Nat. Geosci. 2 (3), 181–184. http://dx.doi.org/10.1038/ngeo437.

Chin, M., Kahn, R.A., Schwartz, S.E., 2009. Atmospheric Aerosol Properties and Climate Impacts. DIANE Publishing, 115 pp.

Christopher, S.A., Wang, J., Ji, Q., Tsay, S.C., 2003. Estimation of diurnal shortwave dust aerosol radiative forcing during PRIDE. J. Geophys. Res. 108, 8596. http://dx.doi.org/10.1029/2002JD002787.

Dubovik, O., King, M.D., 2000. A flexible inversion algorithm for retrieval of aerosol optical properties from Sun and sky radiance measurements. J. Geophys. Res. - Atmos. 105 (D16), 20673–20696. http://dx.doi.org/10.1029/2000JD900282.

Eck, T.F., Holben, B.N., Reid, J.S., Dubovik, O., Smirnov, A., O'Neill, N.T., Slutsker, I., Kinne, S., 1999. Wavelength dependence of the optical depth of biomass burning, urban and desert dust aerosols. J. Geophys. Res. -Atmos. 104, 31333–31350.

Eck, T.F., Holben, B.N., Ward, D.E., Mukelabai, M.M., Dubovik, O., Smirnov, A., Schafer, J.S., Hsu, N.C., Piketh, S.J., Queface, A., Le Roux, J., Swap, R.J., Slutsker, I., 2003. Variability of biomass burning aerosol optical characteristics in southern Africa during the SAFARI 2000 dry season campaign and a comparison of single scattering albedo estimates from radiometric measurements. J. Geophys. Research- Atmos. 108 (D13) http://dx.doi.org/10.1029/2002JD002321.

Gong, C.S., Xin, J.Y., Wang, S.G., Wang, Y.S., Wang, P.C., Wang, L.L., Li, P., 2014. The aerosol direct radiative forcing over the Beijing metropolitan area from 2004 to 2011. J. Aerosol Sci. 69, 62–70.

Guo, J.P., Zhang, X.Y., Che, H.Z., Gong, S.L., An, X.Q., Cao, C.X., 2009. Correlation between PM concentrations and aerosol optical depth in eastern China. Atmos. Environ. 43 (37), 5876–5886. http://dx.doi.org/10.1016/j.atmosenv.2009.08.026.

Guo, J.P., Zhang, X.Y., Wu, Y.R., Zhaxi, Y., Che, H.Z., La, B., Wang, W., Li, X.W., 2011. Spatio-temporal variation trends of satellite-based aerosol optical depth in China during 1980-2008. Atmos. Environ. 45 (37), 6802–6811.

Guo, J.P., Niu, T., Wang, F., Deng, M.J., Wang, Y.Q., 2013. Integration of multi-source measurements to monitor sand-dust storms over North China: a case study. Acta Meteorol. Sin. 27 (4), 566–576. http://dx.doi.org/10.1007/s13351-013-0409-z.

Guo, J.P., Deng, M.J., Fan, J., Li, Z., Chen, Q., Zhai, P.M., Dai, Z., Li, X., 2014. Precipitation and air pollution at mountain and plain stations in northern China: insights gained from observations and modeling. J. Geophys. Res. - Atmos. 119 (8), 4793–4807. http://dx.doi.org/10.1002/2013JD021161.

Guo, J.P., Deng, M.J., Lee, S.-S., Wang, F., Li, Z., Zhai, P.M., Liu, H., Lv, W.T., Yao, W., Li, X., 2016. Delaying precipitation and lightning by air pollution over Pearl River Delta. Part I: observational analyses. J. Geophys. Res. - Atmos. http://onlinelibrary.wiley.com/doi/10.1002/2015JD023257/abstract.

Holben, B.N., Eck, T.F., Slutsker, I., Tanré, D., Buis, J.P., Setzer, A., Vermote, E., Reagan, J.A., Kaufman, Y.J., Nakajima, T., Lavenu, F., Jankowiak, I., Smirnov, A., 1998. AERONET-A federated instrument network and data archive for aerosol characterization. Remote Sens. Environ. 66 (1), 1–16. http://dx.doi.org/10.1016/S0034-4257(98)00031-5.

Kassianov, E., Barnard, J., Pekour, M., Berg, L.K., Michalsky, J., Lantz, K., Hodges, G., 2013. Do diurnal aerosol changes affect daily average radiative forcing? Geophys. Res. Lett. 40 (12), 3265–3269. http://dx.doi.org/10.1002/grl.50567.

Kaufman, Y.J., Tanré, D., Boucher, O., 2002. A satellite view of aerosols in the climate system. Nature 419, 215–223. http://dx.doi.org/10.1038/nature01091.

Keil, A., Haywood, J.M., 2003. Solar radiative forcing by biomass burning aerosol particles during SAFARI 2000: a case study based on measured aerosol and cloud properties. J. Geophys. Res. - Atmos. 108 (D13), 145–160. http://dx.doi.org/10.1029/2002JD002315.

Kotchenova, S.Y., Vermote, E.F., Matarrese, R., Klemm Jr., F.J., 2006. Validation of a vector version of the 6S radiative transfer code for atmospheric correction of satellite data. Part I: path radiance. Appl. Opt. 45, 6762–6774. http://dx.doi.org/10.1364/AO.45.006762.

Kuang, Y., Zhao, C.S., Tao, J.C., Ma, N., 2015. Diurnal variations of aerosol optical properties in the North China Plain and their influences on the estimates of direct aerosol radiative effect. Atmos. Chem. Phys. 15, 5761–5772. http://dx.doi.org/10.5194/acp-15-5761-2015.

Levy, R.C., Remer, L.A., Dubovik, O., 2007. Global aerosol optical properties and application to Moderate Resolution Imaging Spectroradiometer aerosol retrieval over land. J. Geophys. Res. - Atmos. 112, D13210. http://dx.doi.org/10.1029/2006JD007815.

Levy, R.C., Remer, L.A., Kleidman, R.G., Mattoo, S., Ichoku, C., Kahn, R., Eck, T.F., 2010. Global evaluation of the Collection 5 MODIS dark-target aerosol products over land. Atmos. Chem. Phys. 10, 10,399–10,420. http://dx.doi.org/10.5194/acp-10-10399-2010.

Levy, R.C., Mattoo, S., Munchak, L.A., Remer, L.A., Sayer, A.M., Patadia, F., Hsu, N.C., 2013. The Collection 6 MODIS aerosol products over land and ocean. Atmos. Meas. Tech. 6 (11), 2989–3034. http://dx.doi.org/10.5194/amt-6-2989-2013.

Ma, X., Yu, F., 2012. Effect of spectral - dependent surface albedo on Saharan dust direct radiative forcing. Geophys. Res. Lett. 39, L09808. http://dx.doi.org/10.1029/2012GL051360.

Ramanathan, V., Carmichael, G., 2008. Global and regional climate changes due to black carbon. Nat. Geosci. 1, 221–227. http://dx.doi.org/10.1038/ngeo156.

Ramanathan, V., Ramana, M.V., Roberts, G., Kim, D., Corrigan, C.E., Chung, C.E., Winker, D., 2007. Warming trends in Asia amplified by brown cloud solar absorption. Nature 448, 575–578. http://dx.doi.org/10.1038/nature06019.

Remer, L., Kaufman, Y., Tanre, D., Mattoo, S., Chu, D., Martins, J., Li, R.-R., Ichoku, C., Levy, R., Kleidman, R., Eck, T., Vermote, E., Holben, B., 2005. The MODIS aerosol algorithm, products, and validation. J. Atmos. Sci. 62 (4), 947–973.

Salomonson, V.V., Barnes, W., Maymon, P.W., Montgomery, H.E., Ostrow, H., 1989. MODIS: advanced facility instrument for studies of the Earth as a system. IEEE Trans. Geoscience Remote Sens. 27, 145–153. http://dx.doi.org/10.1109/36.20292.

Seinfeld, J., 2008. Atmospheric science - black carbon and brown clouds. Nat. Geosci. 1 (1), 15–16. http://dx.doi.org/10.1038/ngeo.2007.62.

Smirnov, A., Holben, B.N., Eck, T.F., Slutsker, I., Chatenet, B., Pinker, R.T., 2002. Diurnal variability of aerosol optical depth observed at AERONET (Aerosol Robotic Network) sites. Geophys. Res. Lett. 29, 2115. http://dx.doi.org/10.1029/2002GL016305.

Sun, J., Zhang, M., Liu, T., 2001. Spatial and temporal characteristics of dust storms in China and its surrounding regions, 1960–1999: relations to source area and climate. J. Geophys. Res. - Atmos. 106, 10325–10333.

Vermote, E.F., Tanré, D., Deuzé, J.L., Herman, M., Morcrette, J.J., 1997. Second simulation of the satellite signal in the solar spectrum, 6S: an overview. IEEE Trans. Geoscience Remote Sens. 35, 675–686. http://dx.doi.org/10.1109/36.581987.

Wang, F., Guo, J., Zhang, J., Huang, J., Min, M., Chen, T., Liu, H., Deng, M., Li, X., 2015a. Multi-sensor quantification of aerosol-induced variability in warm cloud properties over eastern China. Atmos. Environ. 113, 1–9. http://dx.doi.org/10.1016/j.atmosenv.2015.04.063.

Wang, Z., Liu, D., Wang, Y., Wang, Z., Shi, G., 2015b. Diurnal aerosol variations do affect daily averaged radiative forcing under heavy aerosol loading observed in Hefei China. Atmos. Meas. Tech. 8, 2901–2907. http://dx.doi.org/10.5194/amt-8-2901-2015.

Wu, Y.F., Zhu, J., Che, H., Xia, X., Zhang, R., 2015. Column-integrated aerosol optical properties and direct radiative forcing based on sun photometer measurements at a semi-arid rural site in Northeast China. Atmos. Res. 157, 56–65.

Yin, B.S., Min, Q., 2013. Climatology of aerosol optical properties at ACRF sites in the tropical warm pool region. J. Geophys. Res. - Atmos. 118, 2620–2628. http://dx.doi.org/10.1002/jgrd.50234.

Yoon, S.C., Won, J.G., Omar, A.H., Kim, S.W., Sohn, B.J., 2005. Estimation of the radiative forcing by key aerosol types in worldwide locations using a column model and the AERONET data. Atmos. Environ. 39 (35), 6620–6630. http://dx.doi.org/10.1016/j.atmosenv.2005.07.058.

Yu, H., Kaufman, Y.J., Chin, M., Feingold, G., Remer, L.A., Anderson, T.L., Balkanski, Y., Bellouin, N., Boucher, O., Christopher, S., DeCola, P., Kahn, R., Koch, D., Loeb, N., Reddy, M.S., Schulz, M., Takemura, T., Zhou, M., 2006. A review of measurement-based assessments of the aerosol direct radiative effect and forcing. Atmos. Chem. Phys. 6, 613–666.

Yu, X., Zhu, B., Zhang, M., 2009. Seasonal variability of aerosol optical properties over Beijing. Atmos. Environ. 43, 4095–4101.

Zhang, Y., Yu, H., Eck, T.F., Smirnov, A., Chin, M., Remer, L.A., Bian, H., Tan, Q., Levy, R., Holben, B.N., Piazolla, S., 2012. Aerosol daytime variations over North and South America derived from multiyear AERONET measurements. J. Geophys. Res. - Atmos. 117, D05211. http://dx.doi.org/10.1029/2011JD017242.

Zhuang, B.L., Wang, T.J., Li, S., Liu, J., Talbot, R., Mao, H.T., Yang, X.Q., Fu, C.B., Yin, C.Q., Zhu, J.L., Che, H.Z., Zhang, X.Y., 2014. Optical properties and radiative forcing of urban aerosols in Nanjing, China. Atmos. Environ. 83, 43–52.